MTL TR 92-44

AD

LAU-7/A MISSILE LAUNCHER ATTACHMENT BOLT FAILURES

VICTOR K. CHAMPAGNE, MARC S. PEPI, and
GARY WECHSLER
MATERIALS TESTING AND EVALUATION BRANCH

July 1992

US ARMY
LABORATORY COMMAND
MATERIALS TECHNOLOGY LABORATORY

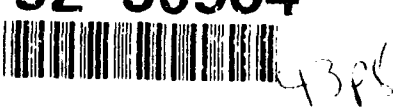

U.S. ARMY MATERIALS TECHNOLOGY LABORATORY
Watertown, Massachusetts 02172-0001

The findings in this report are not to be construed as an official Department of the Army position, unless so designated by other authorized documents.

Mention of any trade names or manufacturers in this report shall not be construed as advertising nor as an official indorsement or approval of such products or companies by the United States Government.

DISPOSITION INSTRUCTIONS

Destroy this report when it is no longer needed.
Do not return it to the originator.

UNCLASSIFIED

SECURITY CLASSIFICATION OF THIS PAGE *(When Data Entered)*

REPORT DOCUMENTATION PAGE		READ INSTRUCTIONS BEFORE COMPLETING FORM
1. REPORT NUMBER MTL-TR-92-44	2. GOVT ACCESSION NO.	3. RECIPIENT'S CATALOG NUMBER
4. TITLE *(and Subtitle)* LAU-7/A MISSILE LAUNCHER ATTACHMENT BOLT FAILURES		5. TYPE OF REPORT & PERIOD COVERED Final Report 6. PERFORMING ORG. REPORT NUMBER
7. AUTHOR*(s)* Victor K. Champagne, Marc S. Pepi, and Gary Wechsler		8. CONTRACT OR GRANT NUMBER*(s)*
9. PERFORMING ORGANIZATION NAME AND ADDRESS U.S. Army Materials Technology Laboratory Watertown, Massachusetts 02172-0001 SLCMT-MRM		10. PROGRAM ELEMENT, PROJECT, TASK AREA & WORK UNIT NUMBERS
11. CONTROLLING OFFICE NAME AND ADDRESS U.S. Army Laboratory Command 2800 Powder Mill Road Adelphi, Maryland 20783-1145		12. REPORT DATE July 1992 13. NUMBER OF PAGES 40
14. MONITORING AGENCY NAME & ADDRESS *(if different from Controlling Office)*		15. SECURITY CLASS. *(of this report)* Unclassified 15a. DECLASSIFICATION/DOWNGRADING SCHEDULE

16. DISTRIBUTION STATEMENT *(of this Report)*

Approved for public release; distribution unlimited.

17. DISTRIBUTION STATEMENT *(of the abstract entered in Block 20, if different from Report)*

18. SUPPLEMENTARY NOTES

19. KEY WORDS *(Continue on reverse side if necessary and identify by block number)*

Missile launcher bolts	Stress corrosion cracking (SCC)
Failure	4340 steel
Metallography	Hy-Tuf steel

20. ABSTRACT *(Continue on reverse side if necessary and identify by block number)*

(SEE REVERSE SIDE)

DD FORM 1 JAN 73 1473 EDITION OF 1 NOV 65 IS OBSOLETE

UNCLASSIFIED

SECURITY CLASSIFICATION OF THIS PAGE *(When Data Entered)*

Block No. 20

ABSTRACT

A comprehensive metallurgical examination of failed LAU-7/A missile launcher attachment bolts was conducted at the U.S. Army Materials Technology Laboratory (MTL) to determine the probable cause of failure. These bolts were utilized to attach LAU-7/A missile launcher systems to Navy F-14 fighter jets.

Light optical microscopy revealed that the fractures occurred at the head to shank radius near the hexagonal recess. Chemical analysis verified the parts were fabricated from the commercially-known *Hy-Tuf* steel. It was determined through metallographic examination that the parts consisted of a typical tempered martensitic structure. Metallography determined that a potentially detrimental surface layer of carburization had been formed during heat treatment. This layer was verified by chemical analysis and microhardness testing. In addition, it was revealed through examination of the macrostructure that the bolts had been machined and not forged as outlined in the governing specification. Fractographic analysis of the crack initiation sites utilizing scanning electron microscopy (SEM) revealed an intergranular mode of fracture, indicative of stress-corrosion cracking (SCC).

It was determined that SCC was the probable cause of failure, and hydrogen charging as a result of surface corrosion was the failure mechanism. Contributing factors to SCC included surface carburization and an unacceptable grain flow pattern. Carburization resulted in a much harder (less tough) surface than was desirable and may have attributed to premature crack initiation while the stress distribution within the bolt head was adversely affected by the improper grain flow.

CONTENTS

INTRODUCTION

The U.S. Navy Pacific Missile Test Center (PMTC) requested the U.S. Army Materials Technology Laboratory (MTL) to investigate the failures of two LAU-7/A launcher attachment bolts that were found to be broken at Oceana, Virginia during preflight inspection. The bolts were fabricated from *Hy-Tuf*,* a high strength, low alloy steel (MIL-S-7108) and were produced to NAVAIRSYSCOM Drawing No. 58A164C57, Revision T. This drawing required the bolts to be heat treated to a hardness of 46.5 to 49.5 Rockwell C, and to be processed in accordance with AMS 7455. The bolts were vacuum cadmium plated to MIL-C-8837, Class 3, Type 2. The washers used in conjunction with the bolts were required to be fabricated from 4130 or 4140 steel and electrolytically cadmium plated to QQ-P-416, Class 2, Type 2 per NAVAIRSYSCOM Drawing No. 58A164B40. The engineering drawings of both the bolt and the washer are shown in Figures 1 and 2. The bolts had been installed on F-14 Navy fighter jets and had been in service approximately two months before failure occurred.

VISUAL EXAMINATION/LIGHT OPTICAL MICROSCOPY

Both failed bolts were stamped on top of the head with the I.D. number 0507 which is the contract number identifying the manufacturer as Chosan, Inc. (see Figures 3a and 3b). Figures 4 and 5 show the two failed launcher attachment bolts identified by MTL as A and B, respectively, in the as-received condition. Both fractures occurred at the head to shank radius near the hexagonal recess. In the case of Bolt B, the primary crack front propagated through the thickness of the material (transversely) until the entire head of the bolt was completely severed, as shown in Figures 3b and 5. During the failure of Bolt A, the main crack front initially proceeded in the same manner but approximately halfway through the bolt, the crack then proceeded in a longitudinal direction until one half of the bolt head became detached from the part as depicted in Figures 3a and 4.

Figures 6 and 7 are schematics of the failed launcher attachment bolts, A and B, respectively, illustrating some of the macro-features revealed on the fracture surfaces and areas adjacent to the failure. Figure 8 shows the Load-Flow line pattern which shows the highest stress to be located at the radius. The principal stress is parallel to the load flow; therefore, the crack front will tend to *run up* perpendicular to the load flow. This process is shown in the insert located at the left hand bottom illustration of Figure 7. Branches B form as the crack attempts to break out. New competing cracks initiate in advance at the radius (the location of the high stress concentration). These cracks link up with the progressing branches and cause steps to form on the resultant fracture surface, as shown in Figure 7. The branches point away from the original crack indicating that the crack origin (primary crack) is that area identified in Figure 7. Confirmation of this conclusion was obtained from the macro-features listed below:

- largest *FLAT* surface area, uninterrupted by stepped topography
- faint radial pattern of micro-steps
- fracture progression lines

After a crack initiates and *runs away* a new one begins at the radius. Hence, there are multiple origins, but most are to be considered as secondary cracks; a feature often associated with stress corrosion cracking (SCC) failures. The link-ups of the secondary cracks with the primary crack front form the many macro-steps observed, especially on the fracture surface of Bolt B.

*Hy-Tuf is a registered trademark of Crucible Materials Corp.

In Figure 7, Branch B broke out to the side and is the same crack as the vertical break A. A similar event caused the vertical break D and E in Figure 6, although in a different manner. In Figure 6, the crack C in the bottom of the hexagonal insert is the same as crack C at the next radius below the head. Its cause is explained in the top left hand schematic.

Examination of the washers used with each bolt revealed damage and wear which corresponded with the deformation contained on the head of the bolts. The washers were determined to have been installed properly on both bolts by matching the wear pattern and damage on the bolts with the washers. It was also noted that the washers could only be seated properly when placed right-side up on the bolt radius (see Figure 9), substantiating the fact that the washers were installed properly. No evidence of extensive corrosion pitting was observed on the outer bolt shank radius. Areas of corrosion were noted on the fracture surfaces and some wear was noted at the radius near the crack origin on both bolts, as Figure 10 shows.

METALLOGRAPHIC EXAMINATION

Macrostructure

A representative 0507 bolt (manufactured by Chosan, Inc.) and a bolt identified as 0437 (manufactured by Production and Tool Co., Inc.) were provided by PMTC for comparative purposes. The two bolts were sectioned longitudinally, and the macrostructure examined. Engineering Drawing 58A184C57 states the "bolt shall be in accordance with AMS 7455E..." AMS 7455E, entitled *Bolts and Screws, Steel, Low-Alloy Heat-Resistant, Hardened and Tempered Roll Threaded* specifies the following (bold added for emphasis):

> *3.2.1 Blanks: Heads shall be formed by **hot forging or cold forging.***

This statement indicates that the bolt heads must not be machined from blanks. Figure 11 illustrates the macrostructural differences between a typical machined and a typical forged bolt head. A further comparison between machined versus forged bolts is listed in the Discussion Section of this analysis.

Figures 12 and 13 show the head region of a longitudinally sectioned 0507 and 0437 bolt, respectively. The samples were etched in a solution consisting of 50% hydrochloric acid and 50% water for 15 minutes. The nature of the flow lines on each sample indicated the bolts were machined and not forged. It was determined the bolts did not conform to 3.4.2.1.1 of AMS 7455E:

> *Examination of a longitudinal section through the part shall show flow lines in the shank, head-to-shank fillet, and bearing surface which follow the contour of the part...*

AMS 7455E also states the following (bold added for emphasis):

> *3.2.5 Thread Rolling: Threads shall be formed on the heat treated and finished blanks by a single **rolling process.***

This statement indicates that the threads must not be ground or cut onto the finished blanks. Figure 14 illustrates the different grain flow pattern between a ground or cut thread

and a rolled thread. A further comparison between cut versus rolled threads is listed in the Discussion Section.

Figures 15 and 16 show the threads of longitudinally sectioned typical 0507 and 0437 bolts, respectively. The samples were etched in a solution consisting of 50% hydrochloric acid and 50% water for 15 minutes. Note the direction of the flow lines within the thread. The flow lines did not follow the contour of the thread, indicative of a cutting or grinding thread forming procedure. It was determined that the bolts did not conform to 3.4.2.1.2 of AMS 7455E:

> *Flow lines in threads shall be continuous, shall follow the general thread contour, and shall be of maximum density at root of thread.*

Microstructure

Bolts A and B were sectioned in the shank region where there was no evidence of wear and Bolt A was also sectioned through the crack origin. These samples were mounted, polished and etched in 1% Nital to reveal the microstructure. Metallographic examination on a Bausch and Lomb research metallograph showed a typical tempered martensitic structure throughout the cores of the cross sections. However, a carburized surface layer (approximately 0.005 inches thick) was revealed as evidenced by a darker etching high carbon martensitic structure (see Figure 17). To verify existence of a carburized surface microhardness testing and chemical analysis were performed within the outside surface layer (approximately 0.020 inches) and compared to that of the core (see chemical analysis and microhardness testing). The microstructure of Bolt A which was sectioned through the crack origin revealed flow lines indicative of a machined (not forged) bolt, as shown in Figure 18. This figure also shows the intergranular fracture surface. A representative 0437 bolt was also examined metallographically. No evidence of carburization was found in this bolt.

The presence of carburization indicated the bolts did not conform to 3.4.3.2 of AMS 7455E, which stated (bold added for emphasis):

> *There shall be no evidence of **carburization**, recarburization, or nitriding.*

CHEMICAL ANALYSIS

Material was sectioned from two different bolts for chemical analysis to establish conformance with drawing requirements and to compare the level of carbon in the surface region. The first bolt chosen for examination was the failed Bolt A and the other was bolt 0437. Pieces of the failed Bolt A (which appeared to have a carburized layer through metallographic and microhardness findings) and Bolt 0437 (which was determined to have little to no carburization) were subjected to chemical analysis. The chemical composition of the bolts was determined by atomic absorption and inductively-coupled argon plasma emission spectrometry. The carbon and sulfur contents were determined by the LECO combustion method. The bolts were sectioned as shown in Figure 19. A disk was sectioned from the shank of each bolt, and the outer 0.020 inches of the disk circumference was removed (see Figure 19) and analyzed separately. The chemical compositional requirements of MIL-S-7108 steel, commercially known as *Hy-Tuf* steel are listed with the chemical composition findings in Table 1.

Table 1. CHEMISTRY COMPARISON

Sample ID	MIL-S-7108	Bolt A Outer Layer	Bolt A Core	0437 Outer Layer	0437 Core
Carbon	0.23 - 0.28	0.394, 0.374*	0.273	0.262	0.260
Sulfur	0.25 Max.	0.008	0.006	0.005	0.003
Manganese	1.20 - 1.50	1.20	1.20	1.36	1.24
Silicon	1.30 - 1.70	1.58	1.54	1.51	1.58
Phosphorus	0.025 Max.	0.014	0.018	0.006	0.006
Chromium	0.40 Max.	0.35	0.35	0.28	0.28
Nickel	1.65 - 2.00	1.78	1.72	1.80	1.74
Molybdenum	0.35 - 0.45	0.41	0.40	0.41	0.39
Copper	---	0.19	0.19	0.094	0.089

*The carbon content of the outer layer of the Bolt A bolt was analyzed twice for verification.

As noted in Table 1, the outer surface of the Bolt A had a much greater carbon content than specified in MIL-S-7108, indicating the presence of a carburized layer, while the core of Bolt A conformed to specification. Both the outer layer and the core of Bolt 0437 satisfied the chemical composition of MIL-S-7108, including the carbon content, indicating that this bolt was not carburized.

FRACTOGRAPHY

Electron microscopy of the crack initiation sites of both bolts revealed an intergranular mode of fracture indicative of a brittle failure (refer to Figure 20). Normal overload failures occurring in this type of material would typically result in a ductile dimpled topography. In order to substantiate this claim, small disc-like cross sections taken from the failed bolt material were bent and broken mechanically in the laboratory and subsequently examined revealing a ductile, dimpled mode of failure indicating that overload conditions would not result in an intergranular fracture like the subject failure. This information also suggested that temper embrittlement had not been the cause of failure since such a condition would also cause an intergranular of failure. Environmentally assisted cracking, such as stress corrosion cracking, often causes failure by intergranular decohesion. The fracture surface of Bolt B failed almost entirely in an intergranular fashion while Bolt A only exhibited an intergranular morphology, primarily within the crack origin regions. Shear lip regions on both failed bolts, (which were the last areas to fracture) exhibited a ductile dimpled mode of failure (refer to Figure 21). There was no evidence indicating that fatigue was the primary cause of failure since there were no distinct beach marks or fatigue striations present.

MICROHARDNESS TESTING

Hardness tests were performed on sections of each of the two failed launcher bolts examined at MTL. The bolts were sectioned, as shown in Figure 22, to obtain both transverse and longitudinal cross sections. Both bolts (Bolt A and B) showed signs of decarburization, as noted previously. Knoop microhardness measurements were performed through the carburized layer transversing into the core of the samples in a step-like manner, as illustrated in Figure 23. The diagonal readings were spaced 0.004 inches in the x-direction and 0.002 inches in the y-direction.

The vertical readings were spaced 0.004 inches apart. The results of this testing are listed in Tables 2 and 3.

Table 2. MICROHARDNESS RESULTS OF BOLT A
KNOOP MICROHARDNESS
20X - 500 gf LOAD
DIAMOND PENETRATOR

Transverse Section			Longitudinal Section		
Reading	Knoop	Eq. HRC	Reading	Knoop	Eq. HRC
1	563	51.0	1	565	51.0
2	545	50.0	2	568	52.0
3	539	50.0	3	549	50.0
4	532	49.5	4	539	50.0
5	504	47.5	5	525	49.0
6	503	47.5	6	490	47.0
7	503	47.5	7	499	47.0
8	500	47.0	8	493	47.0
9	498	47.0	9	487	46.0
10	503	47.5	10	490	47.0

Table 3. MICROHARDNESS RESULTS OF BOLT B
KNOOP MICROHARDNESS
20X - 500 gf LOAD
DIAMOND PENETRATOR

Transverse Section			Longitudinal Section		
Reading	Knoop	Eq. HRC	Reading	Knoop	Eq. HRC
1	574	52.0	1	569	51.5
2	553	51.0	2	552	51.0
3	550	50.5	3	560	51.0
4	532	49.5	4	555	51.0
5	510	48.0	5	541	50.0
6	491	47.0	6	493	47.0
7	490	47.0	7	500	47.5
8	489	47.0	8	494	47.0
9	493	47.0	9	495	47.0
10	490	47.0	10	490	47.0

The hardness near the surface of the bolts was greater (as much as 84 Knoop units, or 5 HRC units) than the hardness in the core. This data substantiates the presence of a carburized layer. According to 3.4.3.2 of AMS 7455E, Vickers hardness readings within 0.003 inches of the surface that are more than 30 points higher than the reading in the core will be evidence of nonconformance to the surface hardening requirement. A difference of 84

Knoop units is equivalent to approximately a difference of 70 Vickers units, at the magnitude of the measured hardness readings (the scale is not linear). Therefore, the carburized bolts did not conform to 3.4.3.2 of AMS 7455E.

EXAMINATION OF ADDITIONAL CONTRACT 0507 BOLTS

To determine the extent that other bolts may have been carburized during heat treatment, a sampling of nine heat treatment lots manufactured under contract 0507 were shipped to the MTL from the PMTC. The lot date, total quantity of bolts from each lot, and the number of samples shipped to MTL are listed in Table 4.

Table 4. LOT SAMPLING INFORMATION

Lot Date	Total Quantity	Shipping Lot	No. MTL Samples
12/90	2,214	1 - 26	5
1/91	1,380	1 - 7	4
2/91	557	1 - 7	2
4/91	1,000	1 - 12	5
5/91	1,222	1 - 15	2
6/4/91	1,260	1 - 26	1
6/24/91	1,307	1 - 16	3
7/91	1,259	1 - 15	2
8/91	1,254	1 - 15	2

The launcher bolts were subsequently sectioned as shown in Figure 24, such that a transverse circular cross section was obtained. These circular sections were mounted and polished before Knoop microhardness measurements were performed in the manner previously described for the failed bolts. The results of this series of microhardness testing are listed in the Appendix. The mounted circular sections were subsequently etched with a 1% Nital solution and examined with the research metallograph to determine the extent of carburization optically. Table 5 is a listing of the bolts examined, the degree of carburization, the range of microhardness and the condition of the bolt (based on microhardness and metallography). A basic rating system was incorporated to classify the extent of carburization on each of the bolts. The intent of this rating system was to determine if the bolts could be placed in service without the risk of premature failure as a result of carburization, only. Representative photomicrographs of three different levels of carburization are shown in Figures 25 through 27.

Table 5. CARBURIZATION OF BOLTS FROM HEAT TREAT LOT SAMPLING AS DETERMINED BY METALLOGRAPHY AND HARDNESS TESTING

Lot Date Bolt I. D.		Degree Of Carburization, Metallography	Hardness Range, Rockwell C (Converted From Knoop Microhardness Readings)	Bolt Condition
12/90 1/26	A	None	47.0 - 48.0	Bolt OK
12/90 16/26	B	None	46.0 - 47.0	Bolt OK
12/90 7/26	C	None	46.5 - 48.0	Bolt OK
12/90 26/26	D	None	46.5 - 47.5	Bolt OK
12/90 17/26	E	None	48.0 - 49.0	Bolt OK
1/91 6/7	A	Heavy	46.0 - 50.5	Bolt Should Not Be Used
1/91 7/7	B	Heavy	46.0 - 50.0	Bolt Should Not Be Used
1/91 7/7	C	Heavy	46.0 - 50.0	Bolt Should Not Be Used
1/91 4/7	D	Heavy	46.0 - 50.0	Bolt Should Not Be Used
2/9 7/7	A	Heavy	45.5 - 49.0	Bolt Should Not Be Used
2/91 4/7	B	Heavy	45.5 - 49.5	Bolt Should Not Be Used
4/91 12/12	A	None to Light	45.0 - 45.5	Bolt Questionable
4/91 12/12	B	None to Light	47.0 - 47.5	Bolt Questionable
4/91 9/12	C	None to Light	47.0 - 49.0	Bolt Questionable
4/91 4/12	D	None to Light	46.5 - 48.0	Bolt Questionable
4/91 8/12	E	None to Light	47.5 - 50.0	Bolt Questionable
5/91 12/15	A	Heavy	45.0 - 50.0	Bolt Should Not Be Used
5/91 6/15	B	Heavy	44.5 - 49.0	Bolt Should Not Be Used
6/91 12/16	A	*Light to Heavy*	46.5 - 50.0	Bolt Should Not Be Used
6/91 12/16	B	Medium	45.5 - 50.0	Bolt Should Not Be Used
6/91 9/16	C	Heavy	45.0 - 50.0	Bolt Should Not Be Used
6/91 12/26	D	Light	47.0 - 48.0	Bolt OK
7/91 2/15	A	Heavy	45.0 - 49.0	Bolt Should Not Be Used
7/91 11/15	B	Light to Heavy	45.0 - 49.0	Bolt Should Not Be Used
8/91 11/15	A	Heavy	46.0 - 50.0	Bolt Should Not Be Used
8/91 11/15	B	Heavy	44.0 - 48.0	Bolt Should Not Be Used

MACROHARDNESS TESTING

Macrohardness tests were performed on the exterior surface of the bolts submitted under contract 0507 to determine if an accurate nondestructive method could be used to test a bolt for carburization. The Rockwell C, 30-N and 15-N scales were employed with little success. The Rockwell C scale (which utilized a 150 kgf major load), the Rockwell 30-N scale (30 kgf major load) and the Rockwell 15-N scale (15 kgf major load) each penetrated through the carburized layer and the resultant measurement represented primarily the core hardness of the bolt; therefore, an accurate assessment of the presence of a carburized layer could not be made. However, a Newage portable hardness tester with a 5 kgf major load (and a minor load of 0.4 kgf) was employed with success in determining the presence of a carburized layer. The cadmium plating was removed chemically, prior to testing to obtain an accurate hardness measurement of the carburized surface region. A stripping solution of ammonium nitrate and water (16 ounces/gallon of water) was employed to remove the cadmium from the end of

each of the bolts. The solution was swabbed over the surface for approximately two minutes, and care was taken to prevent base metal attack. Three hardness readings were measured on each bolt in the location shown in Figure 28. The results are listed in Table 6. Care was also taken to avoid the hardness indents which were present on the bolt from the manufacturer.

Table 6. MACROHARDNESS TESTING DATA TO DETERMINE CARBURIZATION OF BOLTS FROM HEAT TREAT LOT SAMPLING NONDESTRUCTIVELY

Cadmium Plating Removed With Ammonium Nitrate
Hardness Rockwell C
Hardnesses Performed On End Of Bolt
Newage Hardness Tester
5 kgf Major Load, 0.4 kgf Minor Load

Bolt Lot		Reading 1	Reading 2	Reading 3	Average
12/90 1/26	A	49	45	47	47
12/90 16/26	B	47	44	45	45
12/90 7/26	C	45	49	49	48
12/90 26/26	D	49	45	48	47
12/90 17/26	E	45	42	47	45
1/91 6/7	A	49	50	51	50
1/91 7/7	B	52	52	52	52
1/91 7/7	C	53	54	54	54
1/91 4/7	D	52	54	55	54
2/9 7/7	A	52	53	53	53
2/91 4/7	B	52	52	52	52
4/91 12/12	A	52	50	52	51
4/91 12/12	B	54	54	50	53
4/91 9/12	C	53	55	52	53
4/91 4/12	D	46	46	40	47
4/91 8/12	E	54	54	52	53
5/91 12/15	A	49	54	54	52
5/91 6/15	B	55	50	52	52
6/91 12/16	A	49	53	53	52
6/91 12/16	B	55	52	53	53
6/91 9/16	C	50	54	52	52
6/91 12/26	D	45	47	50	47
7/91 2/15	A	52	53	54	53
7/91 11/15	B	49	53	53	52
8/91 11/15	A	52	54	55	54
8/91 11/15	B	51	51	52	51

STRESS DURABILITY TEST

To investigate the possibility that hydrogen may have been introduced into the bolt during the cadmium plating process, and not adequately baked, a stress durability test was performed in accordance with MIL-STD-1312-5A, Test Method 1 (Torque Method). A plate fixture was fabricated from 4340 steel and heat treated to HRC 40. This plate was drilled and tapped to allow

testing of four bolts. These bolts were preloaded to 80% of their ultimate tensile strength (UTS), and subjected to this test for over 200 hours. None of the bolts exhibited signs of fracture when visually examined after completion of the test. These data verify that the bolt failures were not attributed to hydrogen embrittlement as a result of cadmium plating.

DISCUSSION

The fractures of the launcher attachment bolts were brittle in nature, showing little ductility with the exception of the shear lip regions. The morphology of most of the entire fracture surfaces were intergranular in nature while the shear lip regions exhibited a predominantly ductile dimpled topography. When a disc-like piece of material was sectioned from the failed bolt and bent to failure the resulting fracture morphology was dimpled, indicative of a ductile failure. This information along with metallographic examination and hardness testing of the core suggested that the material exhibits ductility when subjected to overload conditions. Therefore, since the crack origin and most of the fracture surface did not display ductility, cracking of both bolts was most likely environmentally assisted.

In addition, the bolts were to be fabricated by hot or cold forming the heads and by rolling the threads. Hot forging, or hot working, entails the plastic deformation of metal at a given temperature and strain rate that allow recrystallization to take place simultaneously with the deformation, thus avoiding any strain hardening. In contrast, cold forging, also known as cold working, involves plastic deformation of metal at temperatures and strain rates which induce strain hardening. The cold forging process is usually, but not necessarily performed at room temperature. Forging, in general, improves bolt strength and integrity by producing uniform, symmetrical grain flow closely following the contour of the head. The low waste and added strength resulting from forging makes it the most accepted and utilized method.

The alternative method of bolt fabrication is the machining process. The primary disadvantage of machining (besides the amount of waste produced) is that cuts are made into the metal grain flow, disrupting optimal stress distribution at the critical head to shank fillet area. This results in a loss of tensile strength and a drastic reduction in tension fatigue performance.

Threads may be added to bolts by either grinding, cutting, or rolling. The optimal method is rolling since the material is forced to flow into the thread contour which is ground into the surface of the die. This produces flow lines within the bolt which follow the contour of the threads, resulting in a stronger thread (rolled threads produce about 40% more holding power than cut threads). Although grinding and cutting are fairly economical, they also present disadvantages. The grain of the metal becomes severed during the grinding and cutting process, and the interrupted grain offers little resistance to the shearing forces which are introduced as a result of mating threads tightening against these cut threads. Both grinding and cutting create chips that may result in a rough surface finish. A rough surface finish can create added points of stress concentration which can lead to fatigue failures in critical applications. In addition, grinding can create cracks in the surface of the fastener and can result in surface burning (and possible alteration of the microstructure of the bolt) if not controlled.

It is well documented that hydrogen assisted cracking occurs in an intergranular fashion in this type of material when heat treated to the hardened condition (HRC 46.5 to 49.5). The

source of hydrogen in this case was probably the result of corrosion. This condition was aggravated by the stress concentration effects of wear at the radius, an unacceptable grain flow pattern and the high notch sensitivity of the material. The carburized surface layer, being more brittle than the core, would also increase the susceptibility to crack initiation.

CONCLUSION

Hydrogen assisted stress corrosion cracking (SCC) was the probable cause of failure in both bolts. Hydrogen charging resulted from surface corrosion. Contributing factors to SCC included surface carburization and an unacceptable grain flow pattern. Carburization resulted in a much harder (less tough) surface than was desirable and may have attributed to premature crack initiation, while the stress distribution within the bolt head was adversely affected by the improper grain flow. Carburization may have accounted for the fact that a significant number of 0507 bolts have experienced field failures, as opposed to those components which exhibited no carburization.

RECOMMENDATIONS

Short Term

The current supply of LAU-7/A launcher attachment bolts manufactured by Chosan, Inc. have been machined and not forged as required; therefore, if new components fabricated to the requirements of NAVAIRSYSCOM Engineering Drawing 58A164C57 Rev. T cannot be procured in a timely fashion, then launcher attachment bolts currently in service that have been determined to be carburized should be replaced with those that are not. MTL has examined samples of bolts from eight heat treat lots representing contract 0507 (provided by the PMTC) and through metallographic examination and hardness testing has concluded that heat treat lot 12/90 does not display evidence of carburization. Heat treat lot 4/91 was found to have a minimal level of carburization optically, but microhardness testing results were to the high side of the acceptable range and macrohardness testing on the exterior surface was similar in value to other carburized heat treat lots (see Tables 5 and 6); therefore, the condition of heat treat lot 4/91 was classified as questionable.

Long Term

The material currently utilized to fabricate the launcher attachment bolts, *Hy-Tuf*, will continue to plague the fleet with similar failures. Action must be taken immediately to either reduce the strength of the bolt (if deemed possible through stress analysis) or to select a new material; i.e., AerMet 100, Inconel 718. Reducing the strength level will improve the notch sensitivity or fracture toughness of the material and increase the resistance to stress corrosion cracking and fatigue. Choosing a different material could accomplish the same results without reducing the current strength level requirements of the bolt. However, when choosing a new material, important aspects must be taken into account to prevent other serious problems from resulting; i.e., galvanic corrosion. In addition, action must be taken to ensure machined bolts are not employed in this application.

Quality Control

Efforts should be made improve quality control and to insure that launcher attachment bolts procured in the future are fabricated according to the requirements of the governing specification. Since two such components attach a LAU-7/A launcher to U.S. Navy fighter jets, it might be feasible to classify these bolts as a critical component. This would allow for traceability of each part to a specific shipping and heat treat lot. In addition, this conversion is made easier by the fact that the bolt is only utilized in conjunction with the LAU-7/A launcher and, therefore, would not impact other noncritical applications.

ACKNOWLEDGMENTS

The authors wish to thank Dr. David Broek for his fractographic analysis in support of this investigation, and Mr. Andrew Zani and Mr. Jack Mullin for their expertise in metallography.

BIBLIOGRAPHY

1. ALLEN, D. K., *Metallurgy Theory and Practice*, American Technical Publishers, Alsip, IL, 1969.

2. ASM Committee on Gas Carburizing, *Carburizing and Carbonitriding*, American Society for Metals, Metals Park, OH, 1977.

3. KRAUSS, G., *Principles of Heat Treatment of Steel*, American Society for Metals, Metals Park, OH, 1980.

4. ASM Handbook Committee, *Properties Selection: Irons and Steels*, Metals Handbook, v. 1, 9th ed., American Society for Metals, Metals Park, OH, 1978.

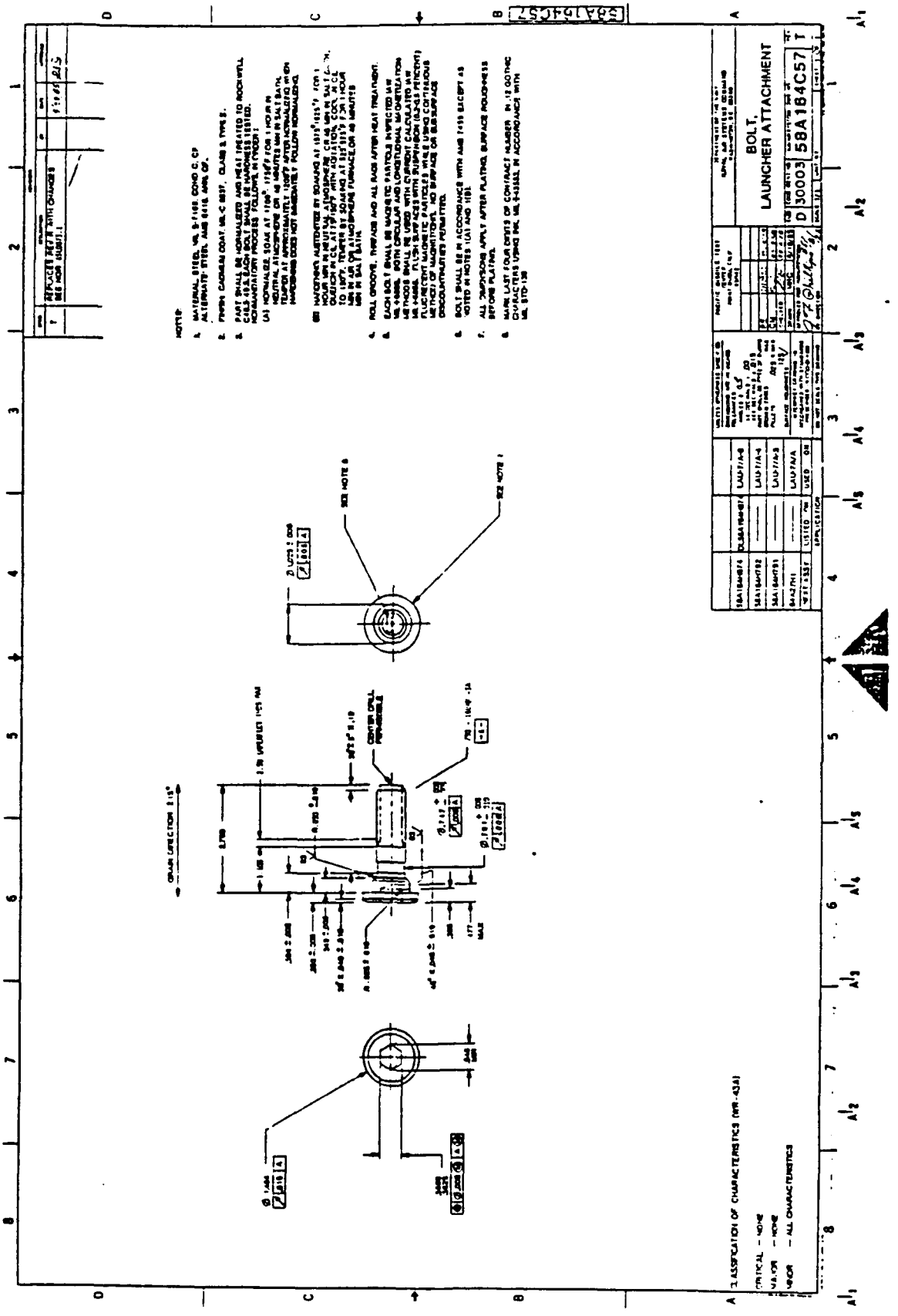

Figure 1. Engineering drawing depicting the LAU-7/A Launcher Attachment Bolt.

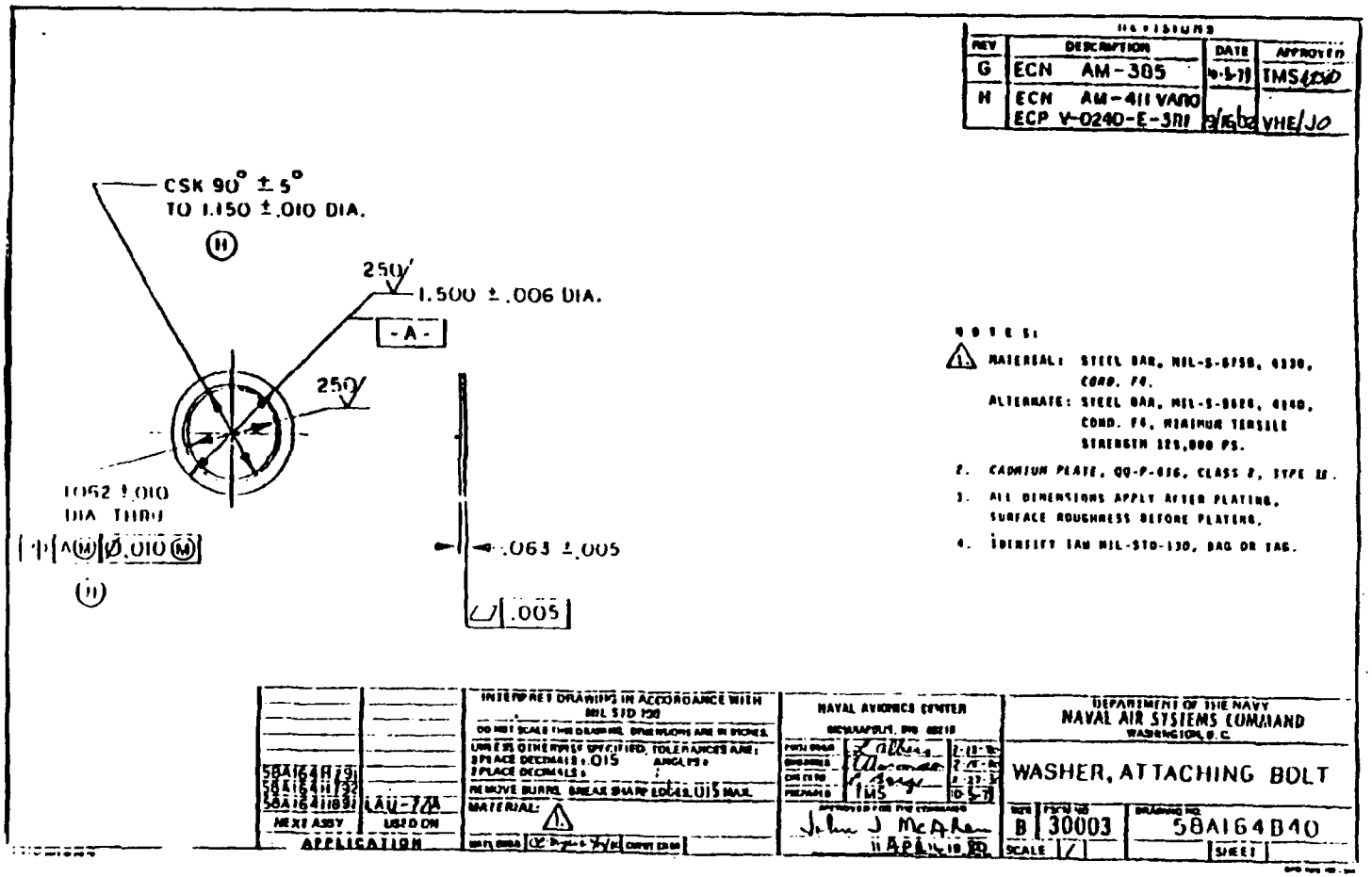

Figure 2. Engineering drawing depicting the washer used in conjunction with the LAU-7/A Launcher Attachment Bolt.

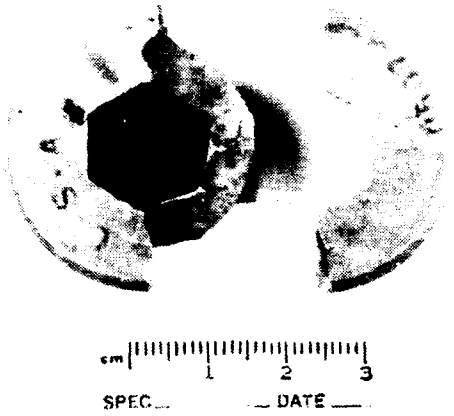

Figure 3a. Macrograph of launcher attachment Bolt A showing the fractured head with the identification number 0507. Reduced 5%.

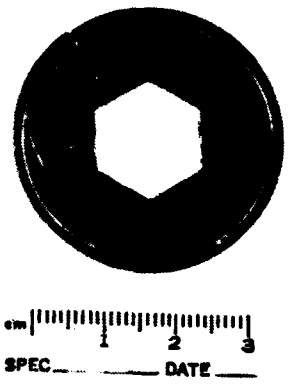

Figure 3b. Macrograph of launcher attachment Bolt B showing the fractured head with the identification number 0507. Reduced 5%.

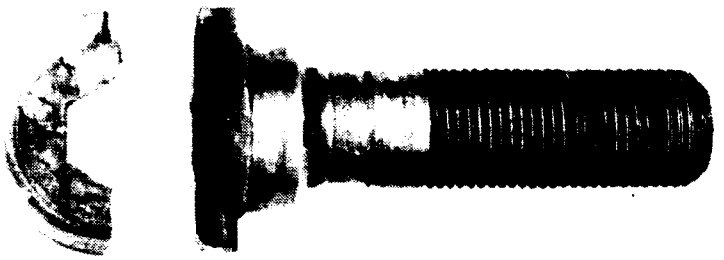

Figure 4. Macrograph showing launcher attachment Bolt A in the as-received condition. Mag. 1X.

Figure 5. Macrograph showing launcher attachment Bolt B in the as-received condition. Mag. 1X.

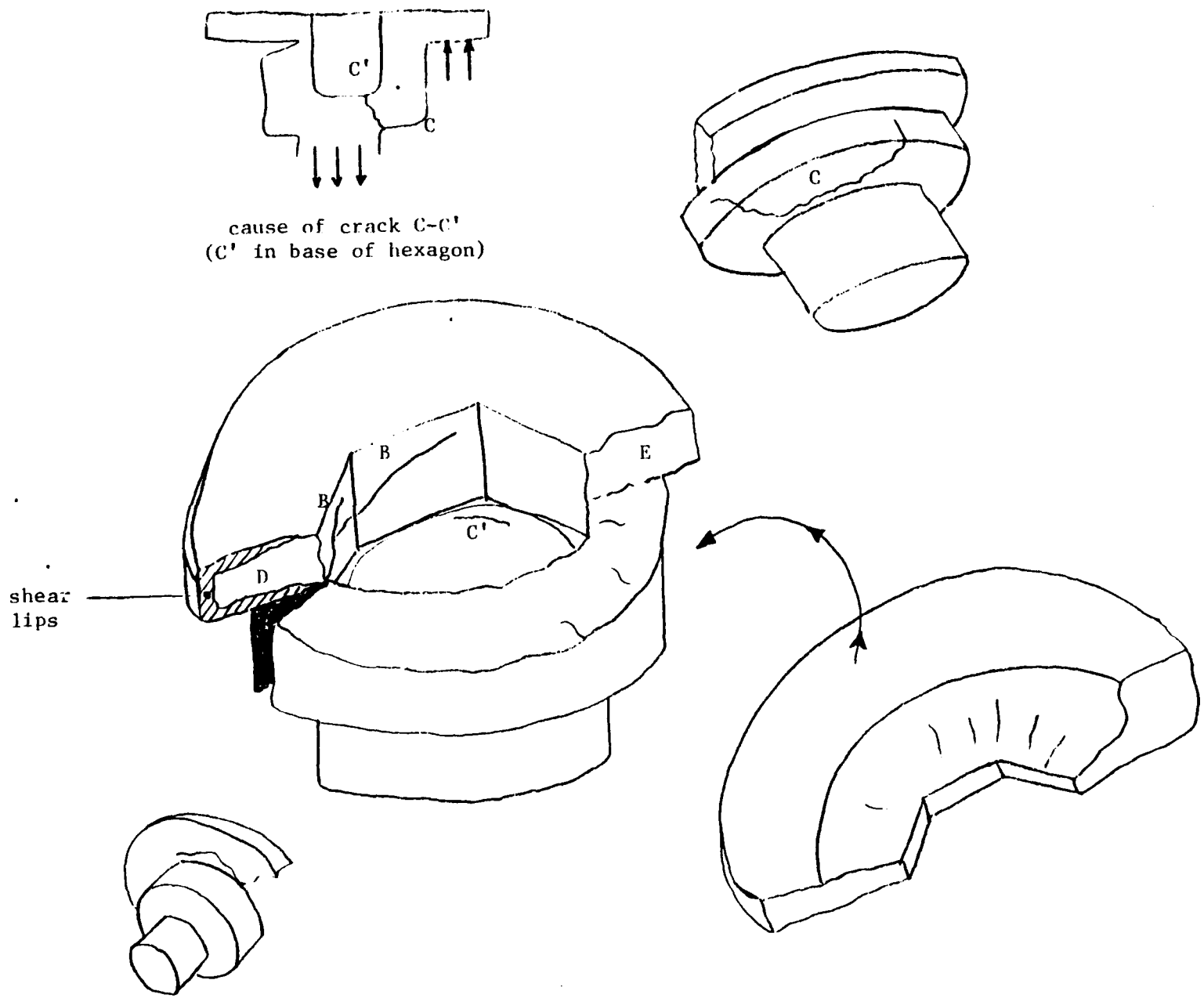

Figure 6. Bolt A failure schematic.

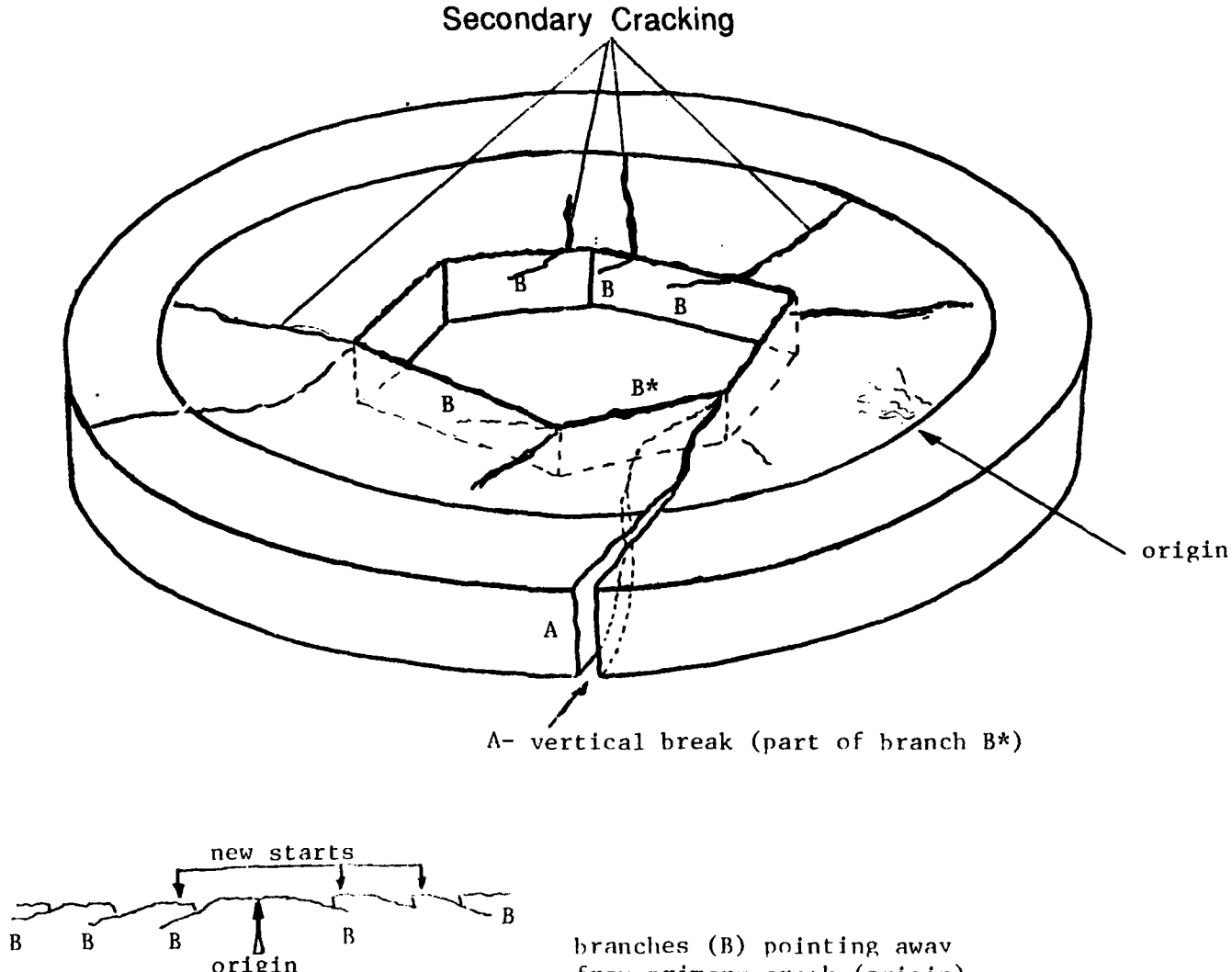

Figure 7. Bolt B failure schematic.

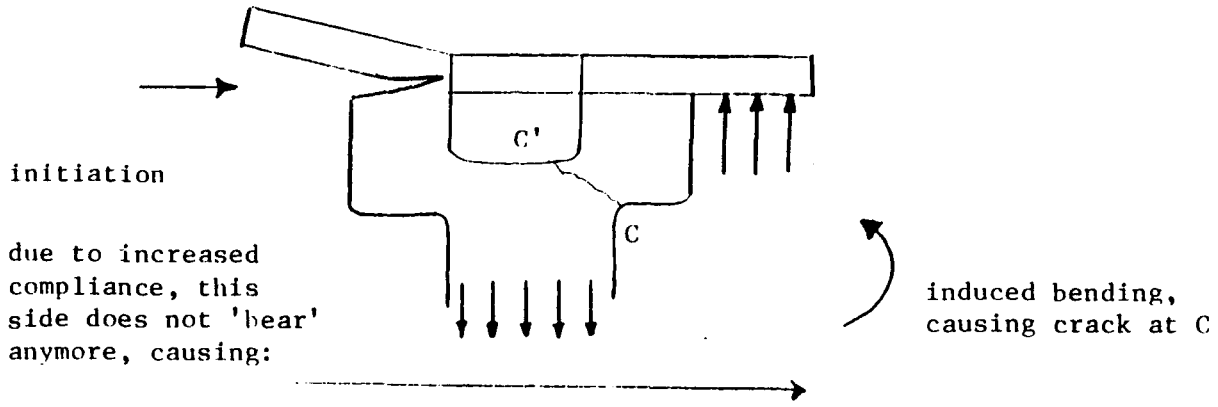

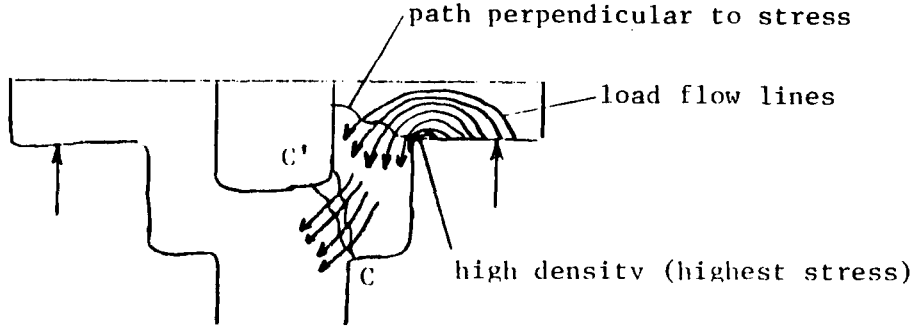

Figure 8. Load flow and stress concentrations.

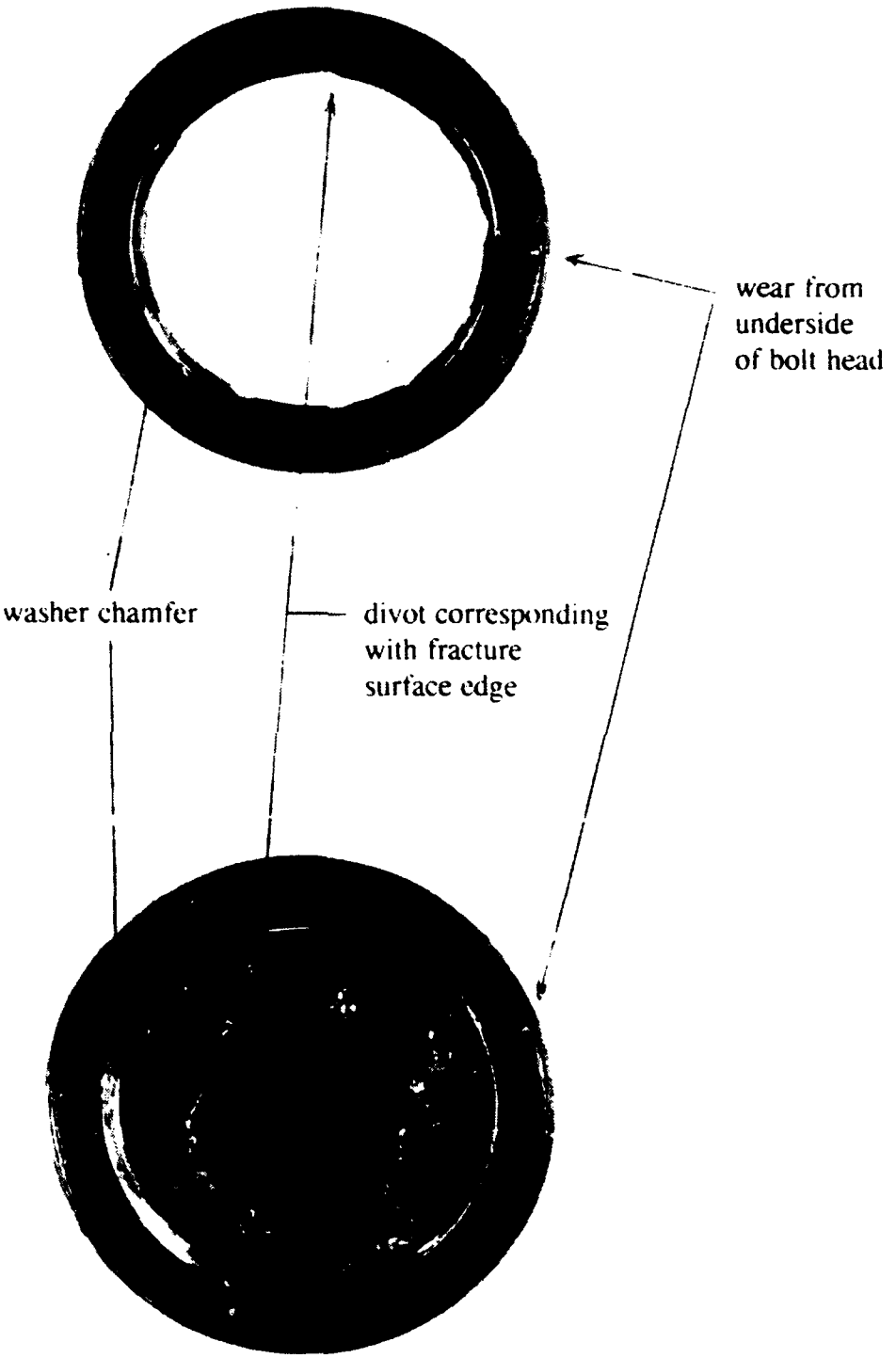

Figure 9. Macrographs showing orientation in which bolt was seated on washer. Mag. 2X.

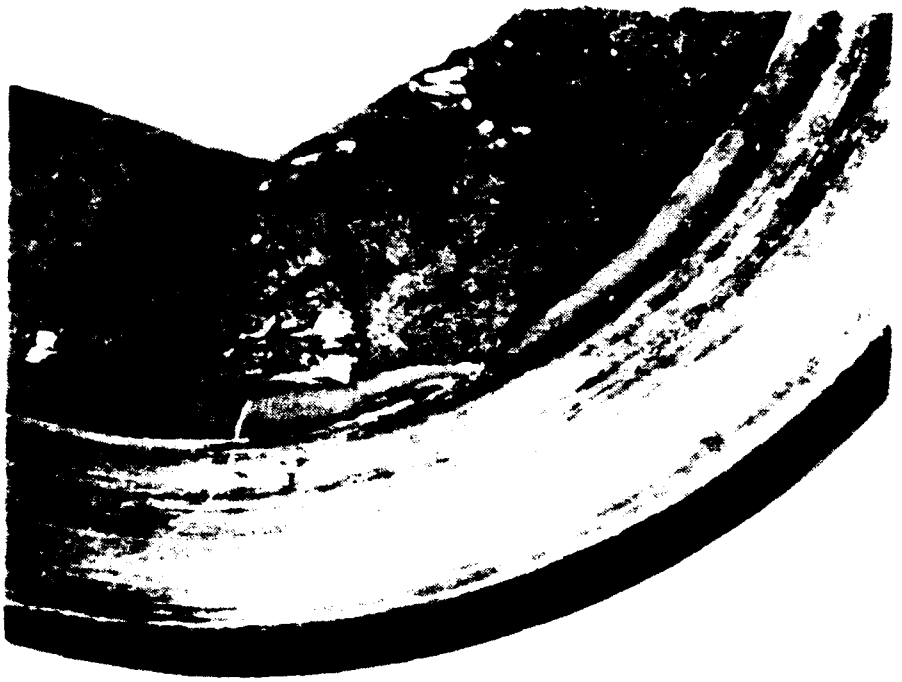

Figure 10. Representative macrograph of the wear noted at the radius near the crack origin of Bolt A. Mag. 7.5X.

Machined Bolt Head

Forged Bolt Head

Figure 11. The macrostructural difference between a typical machined and a typical forged bolt head.

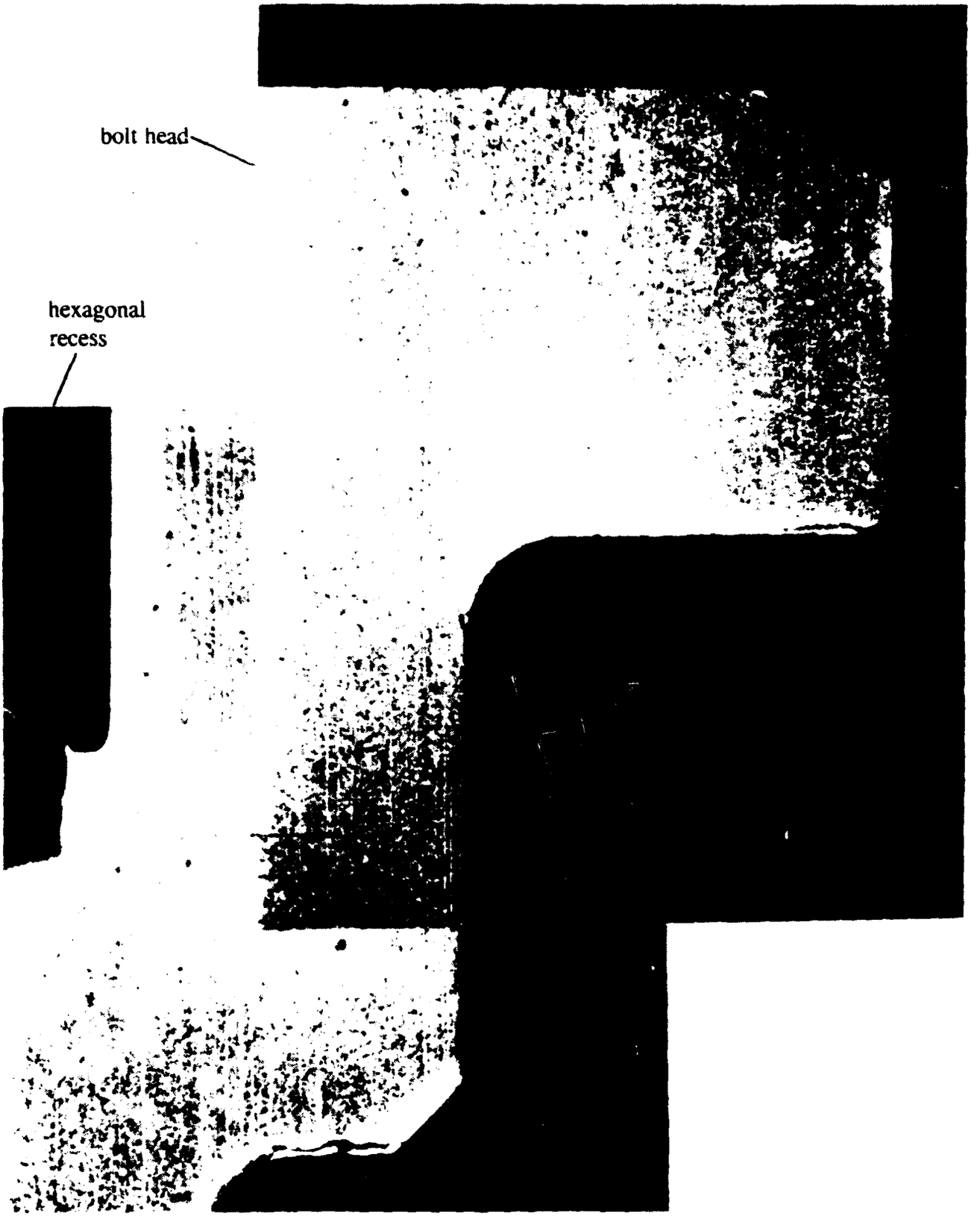

Figure 12. Macrograph of the macrostructure of a representative 0507 bolt head. Flow lines were indicative of a machined bolt head. Mag. 12.5X.

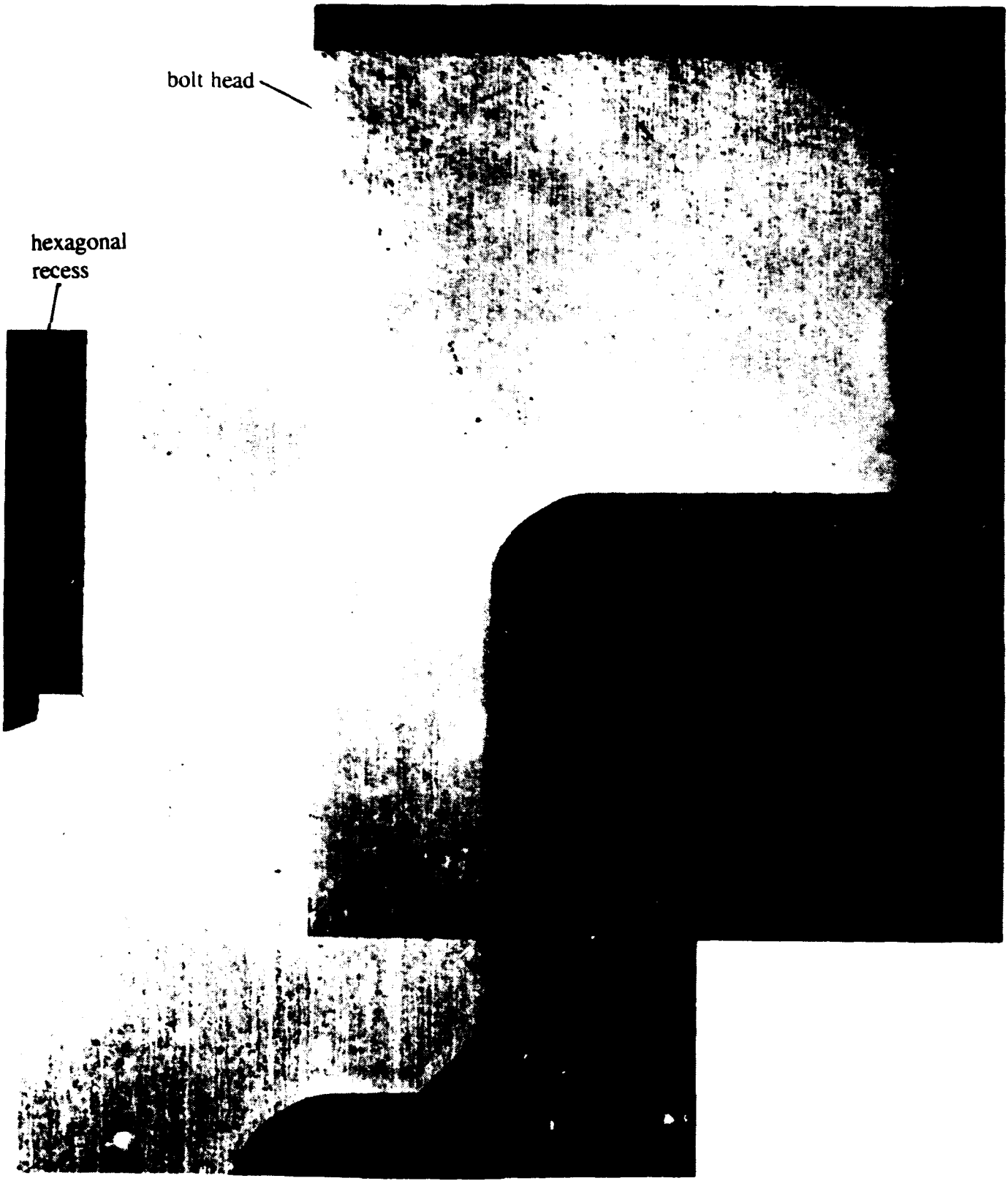

Figure 13. Macrograph of the macrostructure of a representative 0437 bolt head. Flow lines were indicative of a machined bolt head. Mag. 12.5X.

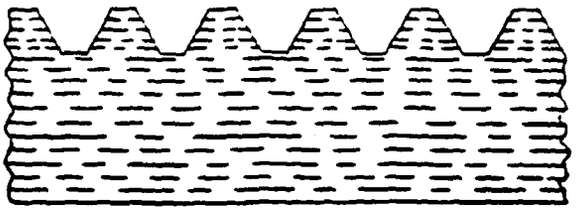

Cut Thread

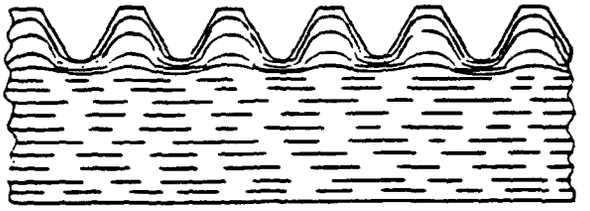

Rolled Thread

Figure 14. Schematic illustrating difference in grain flow pattern between cut versus rolled threads.

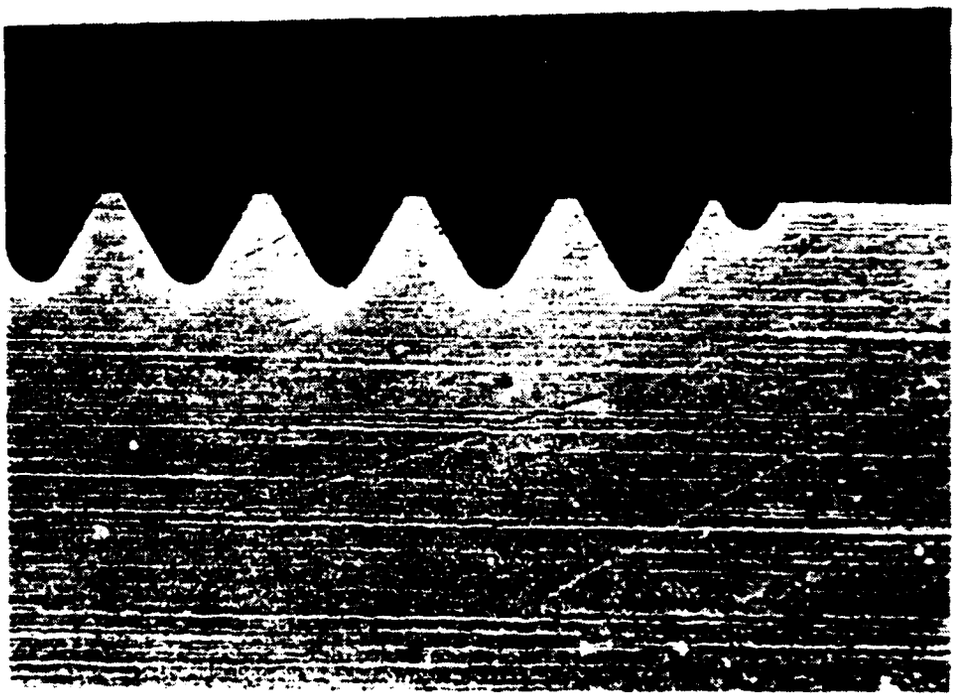

Figure 15. Macrograph of the macrostructure of a representative 0507 bolt thread region. Flow lines were indicative of machined threads. Mag. 12.5X.

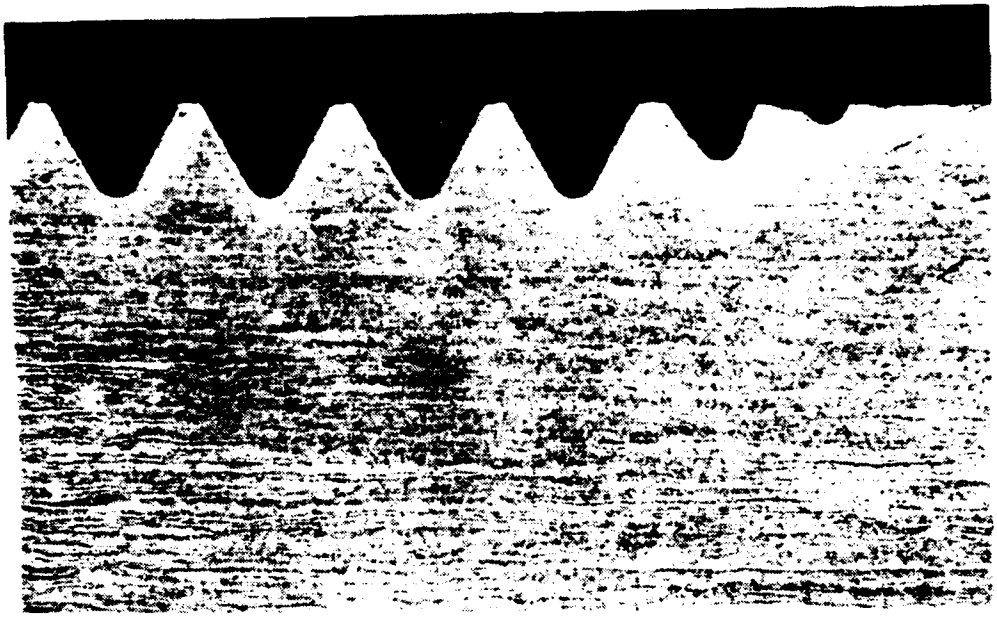

Figure 16. Macrograph of the macrostructure of a representative 0437 bolt thread region. Flow lines were indicative of machined threads. Mag. 12.5X.

Figure 17. Optical micrograph representative of the darker etching high carbon martensitic structure. Mag. 90X.

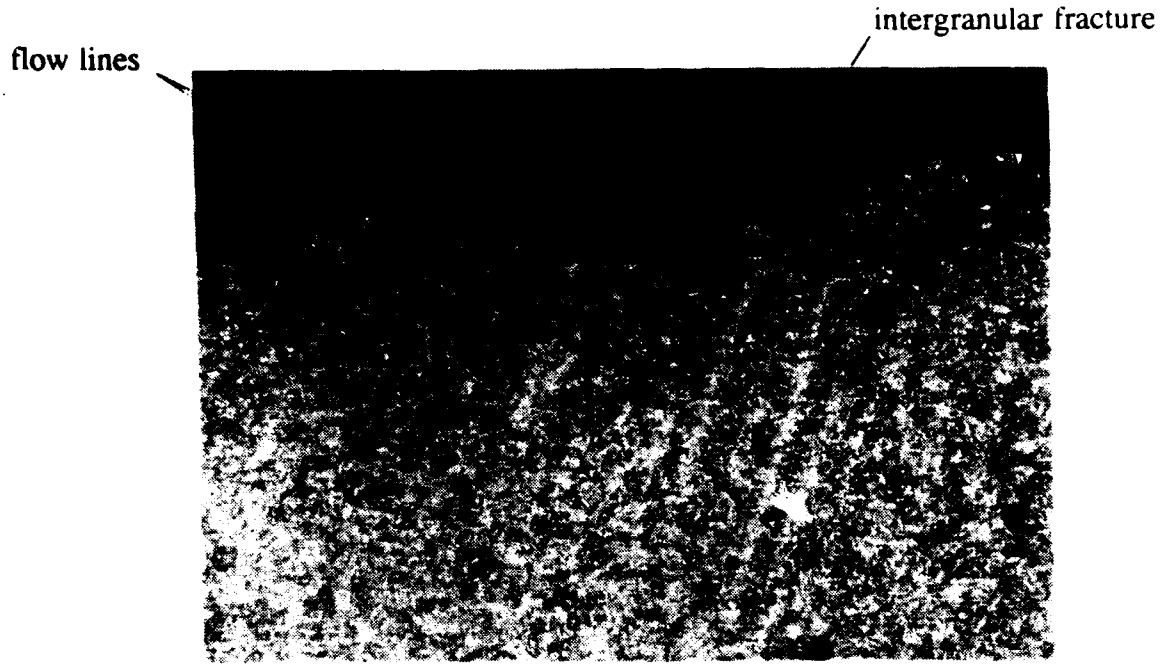

Figure 18. Micrograph of Bolt A which was sectioned through fracture origin. Note intergranular fracture, and the presence of flow lines. Mag. 100X.

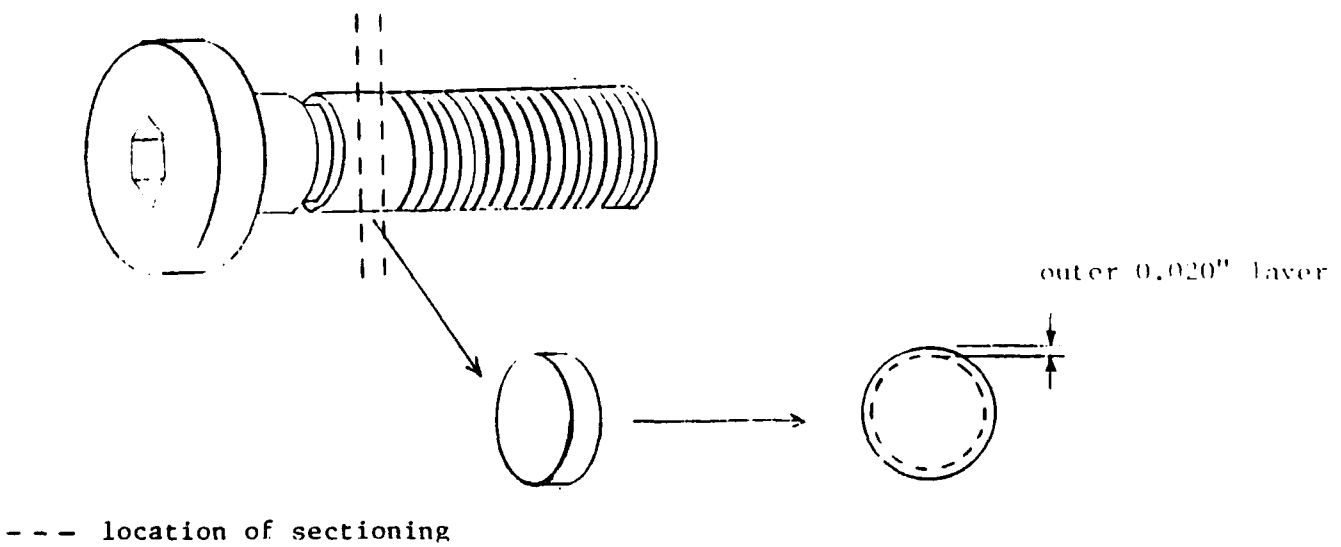

Figure 19. Schematic illustrating sectioning of chemical analysis sample.

Figure 20. SEM showing intergranular mode of failure observed at crack origin and on most of the fracture surface. Mag. 500X.

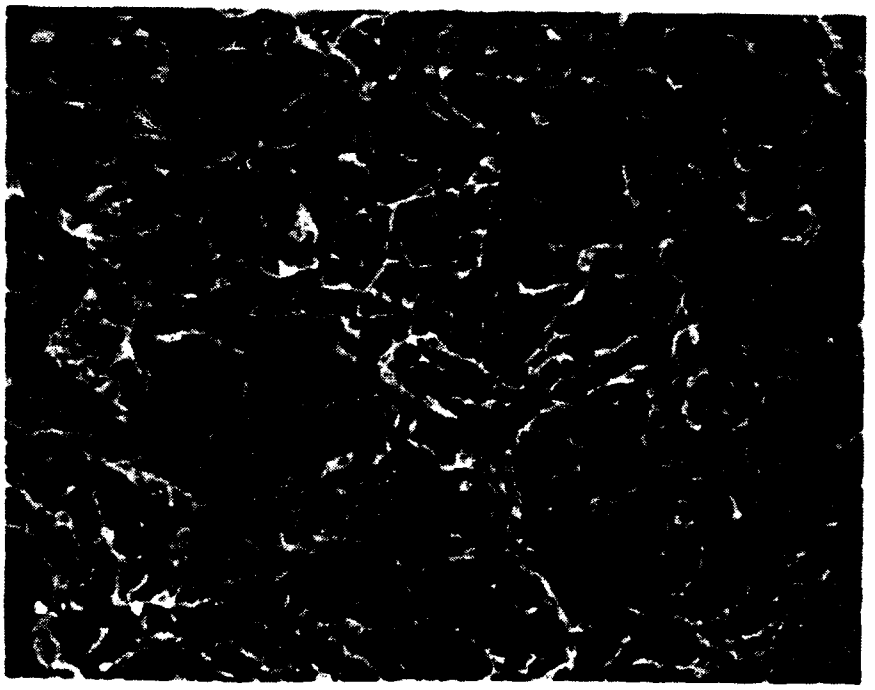

Figure 21. SEM showing ductile, dimpled mode of failure observed on shear lip regions which were the last to fail. Mag. 1500X.

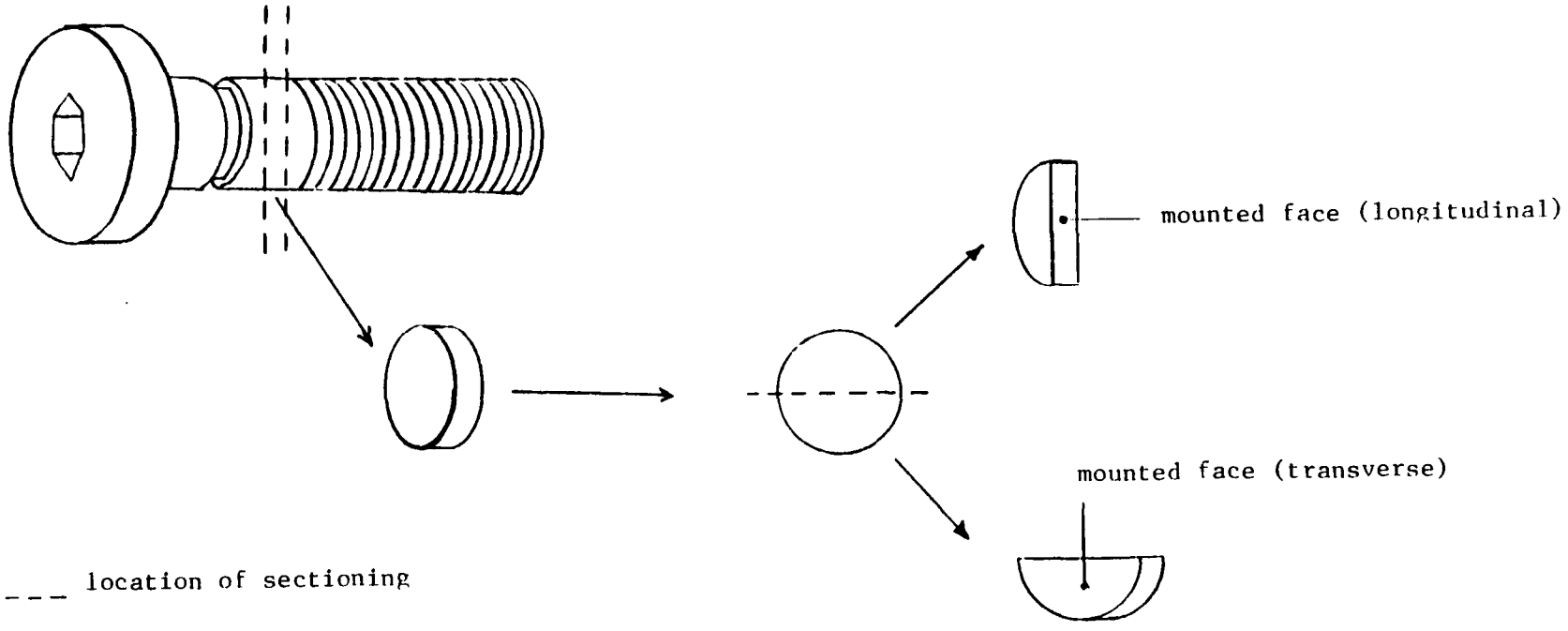

Figure 22. Schematic illustrating method of metallographic sectioning.

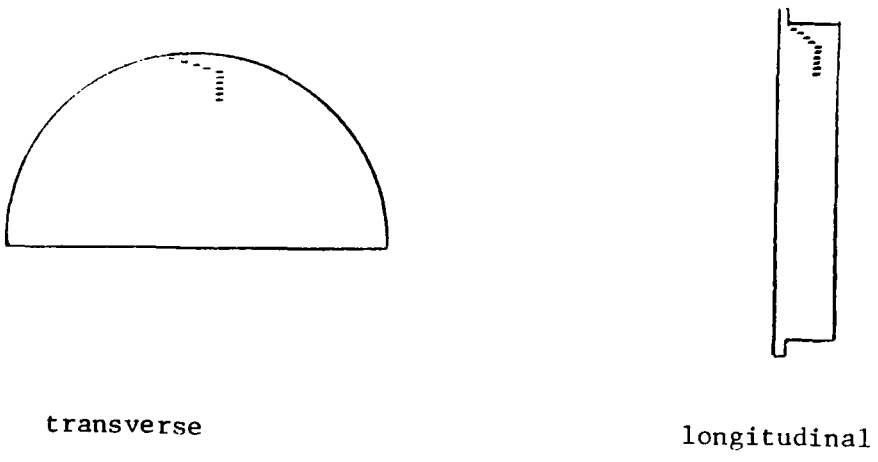

Figure 23. Schematic illustrating location of microhardness measurements on both a transverse and longitudinal sample.

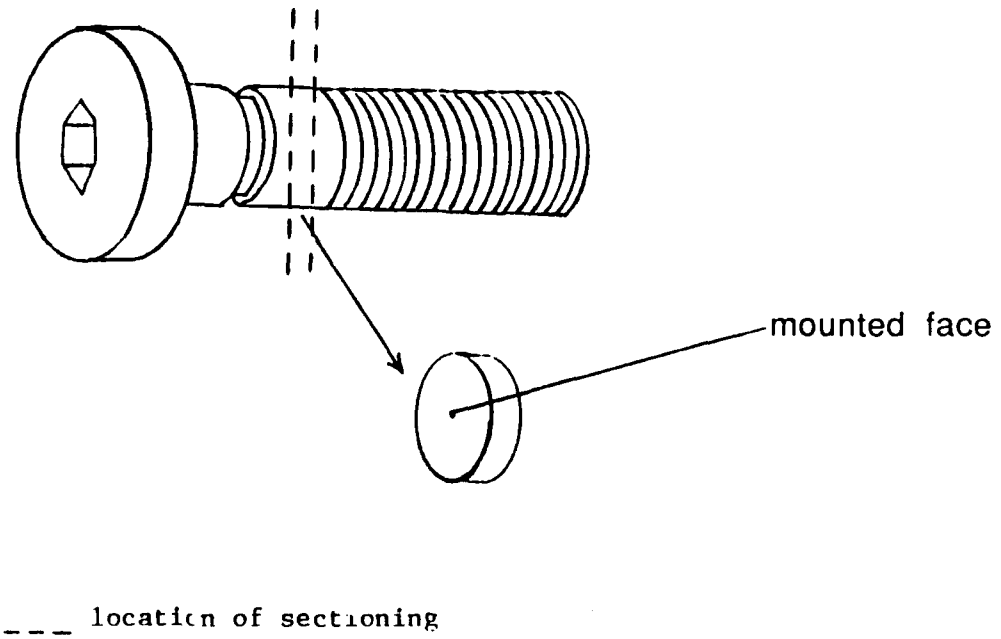

Figure 24. Method of metallographic sample sectioning of sample lot launcher bolts.

Figure 25. Representative micrograph of a *None* to *Light* level of carburization noted on the launcher bolts. Mag. 90X.

Figure 26. Representive micrograph of a *Medium* level of carburization noted on the launcher bolts. Mag. 90X.

Figure 27. Representative micrograph of a *Heavy* level of carburization noted on the launcher bolts. Mag. 90X.

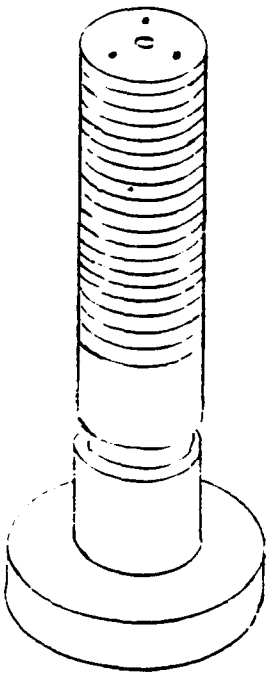

Figure 28. Schematic illustrating location of macrohardness measurements performed on the ends of the launcher bolts.

APPENDIX

Microhardness Testing
Knoop 20X–500g load
Diamond Indentor
12/90 1/26 A

Reading	Knoop	Equiv. HRC
1	492	47.0
2	511	[illegible].0
3	490	[illegible]6.5
4	505	47.5
5	508	48.0
6	505	47.5
7	507	48.0
8	504	47.5
9	497	47.0
10	502	47.5

Microhardness Testing
Knoop 20X–500g load
Diamond Indentor
12/90 16/26 B

Reading	Knoop	Equiv. HRC
1	467	45.0
2	488	46.5
3	492	47.0
4	495	47.0
5	493	47.0
6	496	47.0
7	496	47.0
8	484	46.0
9	485	46.0
10	494	47.0

Microhardness Testing
Knoop 20X–500g load
Diamond Indentor
12/90 7/26 C

Reading	Knoop	Equiv. HRC
1	505	47.5
2	505	47.5
3	515	48.0
4	511	48.0
5	511	48.0
6	507	48.0
7	509	48.0
8	510	48.0
9	487	46.5
10	494	47.0

Microhardness Testing
Knoop 20X–500g load
Diamond Indentor
12/90 26/26 D

Reading	Knoop	Equiv. HRC
1	475	45.5
2	485	46.0
3	487	46.5
4	487	46.5
5	493	47.0
6	502	47.5
7	496	47.0
8	497	47.0
9	496	47.0
10	487	46.5

Microhardness Testing
Knoop 20X–500g load
Diamond Indentor
12/90 17/26 E

Reading	Knoop	Equiv. HRC
1	474	45.5
2	508	48.0
3	497	47.0
4	507	48.0
5	513	48.0
6	521	49.0
7	512	48.0
8	506	48.0
9	512	48.0
10	522	49.0

Microhardness Testing
Knoop 20X–500g load
Diamond Indentor
1/91 6/7 A

Reading	Knoop	Equiv. HRC
1	551	50.5
2	546	50.0
3	531	49.0
4	530	49.0
5	503	47.5
6	502	47.5
7	480	46.0
8	486	46.5
9	486	46.5
10	479	46.0

Microhardness Testing
Knoop 20X–500g load
Diamond Indentor
1/91 7/7 B

Reading	Knoop	Equiv. HRC
1	510	48.0
2	547	50.0
3	531	49.0
4	519	48.5
5	505	47.5
6	488	46.5
7	489	46.5
8	484	46.0
9	482	46.0
10	477	46.0

Microhardness Testing
Knoop 20X–500g load
Diamond Indentor
1/91 7/7 C

Reading	Knoop	Equiv. HRC
1	546	50.0
2	531	49.0
3	519	48.5
4	509	48.0
5	513	48.0
6	486	46.5
7	490	46.5
8	481	46.0
9	489	46.5
10	481	46.0

Microhardness Testing
Knoop 20X–500g load
Diamond Indentor
1/91 4/7 D

Reading	Knoop	Equiv. HRC
1	536	50.0
2	538	50.0
3	524	49.0
4	518	48.5
5	503	47.5
6	490	46.5
7	483	46.0
8	482	46.0
9	472	45.5
10	482	46.0

Microhardness Testing
Knoop 20X–500g load
Diamond Indentor
2/91 7/7 A

Reading	Knoop	Equiv. HRC
1	510	48.0
2	530	49.0
3	521	49.0
4	504	47.5
5	503	47.5
6	485	46.0
7	480	46.0
8	478	46.0
9	473	45.5
10	468	45.0

Microhardness Testing
Knoop 20X–500g load
Diamond Indentor
2/91 4/7 B

Reading	Knoop	Equiv. HRC
1	532	49.5
2	523	49.0
3	523	49.0
4	513	48.0
5	506	48.0
6	495	47.0
7	478	46.0
8	468	45.0
9	474	45.5
10	478	46.0

Microhardness Testing
Knoop 20X–500g load
Diamond Indentor
4/91 12/12 A

Reading	Knoop	Equiv. HRC
1	442	43.0
2	473	45.5
3	469	45.0
4	470	45.0
5	469	45.0
6	466	45.0
7	470	45.0
8	457	44.5
9	468	45.0
10	468	45.0

Microhardness Testing
Knoop 20X–500g load
Diamond Indentor
4/91 12/12 B

Reading	Knoop	Equiv. HRC
1	505	47.5
2	519	48.5
3	494	47.0
4	500	47.5
5	488	46.5
6	493	47.0
7	492	47.0
8	498	47.0
9	503	47.5
10	509	48.0

Microhardness Testing
Knoop 20X–500g load
Diamond Indentor
4/91 9/12 C

Reading	Knoop	Equiv. HRC
1	523	49.0
2	526	49.0
3	523	49.0
4	498	47.0
5	503	47.5
6	496	47.0
7	495	47.0
8	491	47.0
9	496	47.0
10	502	47.5

Microhardness Testing
Knoop 20X–500g load
Diamond Indentor
4/91 4/12 D

Reading	Knoop	Equiv. HRC
1	515	48.0
2	521	49.0
3	508	48.0
4	507	48.0
5	510	48.0
6	496	47.0
7	511	48.0
8	500	47.5
9	495	47.0
10	487	46.5

Microhardness Testing
Knoop 20X–500g load
Diamond Indentor
4/91 8/12 E

Reading	Knoop	Equiv. HRC
1	502	47.5
2	540	50.0
3	532	49.5
4	526	49.0
5	507	48.0
6	499	47.0
7	505	47.5
8	509	48.0
9	502	47.5
10	508	48.0

Microhardness Testing
Knoop 20X–500g load
Diamond Indentor
5/91 12/15 A

Reading	Knoop	Equiv. HRC
1	514	48.0
2	538	50.0
3	523	49.0
4	500	47.5
5	502	47.5
6	486	46.5
7	478	46.0
8	477	46.0
9	474	45.5
10	471	45.0

Microhardness Testing
Knoop 20X–500g load
Diamond Indentor
5/91 6/15 B

Reading	Knoop	Equiv. HRC
1	516	48.0
2	527	49.0
3	494	47.0
4	477	46.0
5	467	45.0
6	451	44.0
7	451	44.0
8	462	45.0
9	461	44.5
10	457	44.5

Microhardness Testing
Knoop 20X–500g load
Diamond Indentor
6/91 12/12 A

Reading	Knoop	Equiv. HRC
1	519	48.5
2	538	50.0
3	527	49.0
4	515	48.0
5	507	48.0
6	493	47.0
7	490	46.5
8	490	46.5
9	498	47.0
10	488	46.5

Microhardness Testing
Knoop 20X–500g load
Diamond Indentor
6/91 12/16 B

Reading	Knoop	Equiv. HRC
1	542	50.0
2	531	49.0
3	514	48.0
4	493	47.0
5	497	47.0
6	484	46.0
7	476	46.0
8	468	45.0
9	476	46.0
10	474	45.5

Microhardness Testing
Knoop 20X–500g load
Diamond Indentor
6/91 9/16 C

Reading	Knoop	Equiv. HRC
1	546	50.0
2	547	50.0
3	526	49.0
4	511	48.0
5	497	47.0
6	472	45.5
7	473	45.5
8	481	46.0
9	467	45.0
10	470	45.0

Microhardness Testing
Knoop 20X–500g load
Diamond Indentor
6/91 12/26 D

Reading	Knoop	Equiv. HRC
1	475	45.5
2	482	46.0
3	512	48.0
4	512	48.0
5	499	47.0
6	520	48.5
7	514	48.0
8	512	48.0
9	505	47.5
10	499	47.0

Microhardness Testing
Knoop 20X – 500g load
Diamond Indentor
7/91 2/15 A

Reading	Knoop	Equiv. HRC
1	523	49.0
2	493	47.0
3	489	46.5
4	482	46.0
5	469	45.0
6	463	45.0
7	463	45.0
8	472	45.5
9	466	45.0
10	473	45.5

Microhardness Testing
Knoop 20X – 500g load
Diamond Indentor
7/91 11/15 B

Reading	Knoop	Equiv. HRC
1	490	46.5
2	501	47.5
3	521	49.0
4	493	47.0
5	463	45.0
6	464	45.0
7	470	45.0
8	475	45.5
9	472	45.5
10	478	46.0

Microhardness Testing
Knoop 20X – 500g load
Diamond Indentor
8/91 11/15 A

Reading	Knoop	Equiv. HRC
1	547	50.0
2	524	49.0
3	528	49.0
4	515	48.0
5	490	46.5
6	487	46.5
7	489	46.5
8	476	46.0
9	480	46.0
10	485	46.0

Microhardness Testing
Knoop 20X – 500g load
Diamond Indentor
8/91 11/15 B

Reading	Knoop	Equiv. HRC
1	501	47.5
2	508	48.0
3	484	46.0
4	479	46.0
5	460	44.5
6	450	44.0
7	456	44.0
8	448	44.0
9	446	44.0
10	459	44.5

DISTRIBUTION LIST

No. of Copies	To
1	Office of the Under Secretary of Defense for Research and Engineering, The Pentagon, Washington, DC 20301
	Commander, Defense Technical Information Center, Cameron Station, Bldg. 5, 5010 Duke Street, Alexandria VA 22304-6145
2	ATTN: DTIC-FDAC
1	MIAC/CINDAS, Purdue University, 2595 Yeager Road, West Lafayette, IN 47905
	Commander, U.S. Army Materiel Command, 5001 Eisenhower Avenue, Alexandria, VA 22333
1	ATTN: AMCSCI
1	AMCQA-P, S. J. Lorber
	Commander, Pacific Missile Test Center, Point Mugu, CA 93042
1	ATTN: John Durda, Code 2041
1	Carl Louck, Code 2041
1	John Piercy, Code 2041
1	Sam Keller, Code 2043
1	Bill Mcauley, Code 2043
	Commander, U.S. Army Laboratory Command, 2800 Powder Mill Road, Adelphi, MD 20783-1145
1	ATTN: AMSLC-IM-TL
1	AMSLC-CT
	Commander, Rock Island Arsenal, Headquarters AMCCOM, Rock Island, IL 61299-6000
1	ATTN: AMSMC-PCA-WM, Joe Wells
1	AMSMC-QAM-I, Gary Smith
1	AMSMC-ASR-M, Brian Kunkel
1	John Housseman
	Commander, U.S. Army Test and Evaluation Command, Aberdeen Proving Ground, MD 21005
1	ATTN: Library
1	Clarke Engineer School Library, 3202 Nebraska Ave. North, Ft. Leonard Wood, MO 65473-5000
	Naval Air System Command, Department of the Navy, Washington, DC 20360
1	ATTN: AIR-03PAF
	Naval Research Laboratory, Washington, DC 20375
1	ATTN: Code 5830
	Naval Air Development Center, Warminster, PA 18974
1	ATTN: Code 063
	Commander, U.S. Army Aviation Systems Command (AVSCOM) St. Louis, MO 63120-1798
1	ATTN: AMSAV-ECC, Emanuel Buelter
1	AMSAV-ECC, Robert Lawyer
1	AMSAV-EFM, Frank Barhorst
1	AMSAV-EFM, Kirit Bhansali
1	AMSAV-E, Carl Smith
1	AMCPM-AAH, Dave Roby
1	AMCPM-AAH, Bob Kennedy
	Commander, Corpus Christi Army Depot, Corpus Christi, TX 78419-6195
1	ATTN: AMSAV-MRPD, Nicholas Hurta, Mail Stop 55
1	AMSAV-MRPD, Lou Neri, Mail Stop 55
1	SDSCC-QLM, David Garcia, Mail Stop 27
1	SDSCC-QLM, Charlie Wilson, Mail Stop 27
	Commander, Armament Research, Development and Engineering Center, Picatinny Arsenal, NJ 07806-5000
1	ATTN: SMCAR-CCS-C, Anthony Sebasto, Bldg. #1
	Program Manager, Government-Industry Data Exchange, GIDEP Operations Center, Corona, CA 91720-2000
1	ATTN: J. C. Richards, Program Director
	Director, U.S. Army Materials Technology Laboratory, Watertown, MA 02172-0001
2	ATTN: SLCMT-TML
3	Authors

U.S. Army Materials Technology Laboratory
Watertown, Massachusetts 02172-0001
LAU-7/A MISSILE LAUNCHER ATTACHMENT BOLT FAILURES -
Victor K. Champagne, Marc S. Pepi, and Gary Wechsler

Technical Report MTL TR 92-44, June 1992, 40 pp-
illus-tables,

AD__________
UNCLASSIFIED
UNLIMITED DISTRIBUTION

KeyWords
Missile launcher bolts
Failure
Metallography

A comprehensive metallurgical examination of failed LAU-7/A missile launcher attachment bolts was conducted at the U.S. Army Materials Technology Laboratory (MTL) to determine the probable cause of failure. These bolts were utilized to attach LAU-7/A missile launcher systems to Navy F-14 fighter jets. Light optical microscopy revealed that the fractures occurred at the head to shank radius near the hexagonal recess. Chemical analysis verified the parts were fabricated from the commercially-known *Hy-Tuf* steel. It was determined through metallographic examination that the parts consisted of a typical tempered martensitic structure. Metallography determined that a potentially detrimental surface layer of carburization had been formed during heat treatment. This layer was verified by chemical analysis and microhardness testing. In addition, it was revealed through examination of the macrostructure that the bolts had been machined and not forged as outlined in the governing specification. Fractographic analysis of the crack initiation sites utilizing scanning electron microscopy (SEM) revealed an intergranular mode of fracture, indicative of stress-corrosion cracking (SCC). It was determined that SCC was the probable cause of failure, and hydrogen charging as a result of surface corrosion was the failure mechanism. Contributing factors to SCC included surface carburization and an unacceptable grain flow pattern. Carburization resulted in a much harder (less tough) surface than was desirable and may have attributed to premature crack initiation while the stress distribution within the bolt head was adversely affected by the improper grain flow.

U.S. Army Materials Technology Laboratory
Watertown, Massachusetts 02172-0001
LAU-7/A MISSILE LAUNCHER ATTACHMENT BOLT FAILURES -
Victor K. Champagne, Marc S. Pepi, and Gary Wechsler

Technical Report MTL TR 92-44, June 1992, 40 pp-
illus-tables,

AD__________
UNCLASSIFIED
UNLIMITED DISTRIBUTION

KeyWords
Missile launcher bolts
Failure
Metallography

A comprehensive metallurgical examination of failed LAU-7/A missile launcher attachment bolts was conducted at the U.S. Army Materials Technology Laboratory (MTL) to determine the probable cause of failure. These bolts were utilized to attach LAU-7/A missile launcher systems to Navy F-14 fighter jets. Light optical microscopy revealed that the fractures occurred at the head to shank radius near the hexagonal recess. Chemical analysis verified the parts were fabricated from the commercially-known *Hy-Tuf* steel. It was determined through metallographic examination that the parts consisted of a typical tempered martensitic structure. Metallography determined that a potentially detrimental surface layer of carburization had been formed during heat treatment. This layer was verified by chemical analysis and microhardness testing. In addition, it was revealed through examination of the macrostructure that the bolts had been machined and not forged as outlined in the governing specification. Fractographic analysis of the crack initiation sites utilizing scanning electron microscopy (SEM) revealed an intergranular mode of fracture, indicative of stress-corrosion cracking (SCC). It was determined that SCC was the probable cause of failure, and hydrogen charging as a result of surface corrosion was the failure mechanism. Contributing factors to SCC included surface carburization and an unacceptable grain flow pattern. Carburization resulted in a much harder (less tough) surface than was desirable and may have attributed to premature crack initiation while the stress distribution within the bolt head was adversely affected by the improper grain flow.

U.S. Army Materials Technology Laboratory
Watertown, Massachusetts 02172-0001
LAU-7/A MISSILE LAUNCHER ATTACHMENT BOLT FAILURES -
Victor K. Champagne, Marc S. Pepi, and Gary Wechsler

Technical Report MTL TR 92-44, June 1992, 40 pp-
illus-tables,

AD__________
UNCLASSIFIED
UNLIMITED DISTRIBUTION

KeyWords
Missile launcher bolts
Failure
Metallography

A comprehensive metallurgical examination of failed LAU-7/A missile launcher attachment bolts was conducted at the U.S. Army Materials Technology Laboratory (MTL) to determine the probable cause of failure. These bolts were utilized to attach LAU-7/A missile launcher systems to Navy F-14 fighter jets. Light optical microscopy revealed that the fractures occurred at the head to shank radius near the hexagonal recess. Chemical analysis verified the parts were fabricated from the commercially-known *Hy-Tuf* steel. It was determined through metallographic examination that the parts consisted of a typical tempered martensitic structure. Metallography determined that a potentially detrimental surface layer of carburization had been formed during heat treatment. This layer was verified by chemical analysis and microhardness testing. In addition, it was revealed through examination of the macrostructure that the bolts had been machined and not forged as outlined in the governing specification. Fractographic analysis of the crack initiation sites utilizing scanning electron microscopy (SEM) revealed an intergranular mode of fracture, indicative of stress-corrosion cracking (SCC). It was determined that SCC was the probable cause of failure, and hydrogen charging as a result of surface corrosion was the failure mechanism. Contributing factors to SCC included surface carburization and an unacceptable grain flow pattern. Carburization resulted in a much harder (less tough) surface than was desirable and may have attributed to premature crack initiation while the stress distribution within the bolt head was adversely affected by the improper grain flow.

U.S. Army Materials Technology Laboratory
Watertown, Massachusetts 02172-0001
LAU-7/A MISSILE LAUNCHER ATTACHMENT BOLT FAILURES -
Victor K. Champagne, Marc S. Pepi, and Gary Wechsler

Technical Report MTL TR 92-44, June 1992, 40 pp-
illus-tables,

AD__________
UNCLASSIFIED
UNLIMITED DISTRIBUTION

KeyWords
Missile launcher bolts
Failure
Metallography

A comprehensive metallurgical examination of failed LAU-7/A missile launcher attachment bolts was conducted at the U.S. Army Materials Technology Laboratory (MTL) to determine the probable cause of failure. These bolts were utilized to attach LAU-7/A missile launcher systems to Navy F-14 fighter jets. Light optical microscopy revealed that the fractures occurred at the head to shank radius near the hexagonal recess. Chemical analysis verified the parts were fabricated from the commercially-known *Hy-Tuf* steel. It was determined through metallographic examination that the parts consisted of a typical tempered martensitic structure. Metallography determined that a potentially detrimental surface layer of carburization had been formed during heat treatment. This layer was verified by chemical analysis and microhardness testing. In addition, it was revealed through examination of the macrostructure that the bolts had been machined and not forged as outlined in the governing specification. Fractographic analysis of the crack initiation sites utilizing scanning electron microscopy (SEM) revealed an intergranular mode of fracture, indicative of stress-corrosion cracking (SCC). It was determined that SCC was the probable cause of failure, and hydrogen charging as a result of surface corrosion was the failure mechanism. Contributing factors to SCC included surface carburization and an unacceptable grain flow pattern. Carburization resulted in a much harder (less tough) surface than was desirable and may have attributed to premature crack initiation while the stress distribution within the bolt head was adversely affected by the improper grain flow.